Observation of a Textural Transformation Associated with the A_2 Transition in Superfluid ^{3}He-A

P. G. N. de Vegvar,[a] R. Movshovich, E. L. Ziercher, and D. M. Lee
Laboratory of Atomic and Solid State Physics, Cornell University, Ithaca, New York 14853
(Received 24 January 1986)

We have observed an anomaly in the attenuation and phase velocity of zero sound in superfluid ^{3}He-A at a temperature experimentally unresolvable from the A_2 transition. The feature is present at all magnetic fields and frequencies for sound propagated perpendicular to the applied field **H**, but it disappears for sound traveling along **H**. We discuss this phenomenon in terms of a *first*-order transformation between dipole-locked and dipole-unlocked planar textures driven by the thermodynamic *second*-order phase transition at T_{A_2}. We also report the first observed splitting of the normal flapping mode in a magnetic field.

PACS numbers: 67.50.Fi, 64.70.–p, 67.40.Pm

For many years ultrasound has been used as a probe of the order parameter of superfluid ^{3}He.[1] In this work we report on measurements of zero-sound propagation in ^{3}He-A in magnetic fields up to 94 kG. This region of the phase diagram has only recently become experimentally accessible. In addition to observing the expected splitting of the collective modes due to the unequal gaps in the two spin bands,[2] we have intensively studied an anomaly that appears very close to the A_2 transition. Although this feature was first inferred from earlier experiments,[3] the current research has led to a deeper understanding of the phenomenon.

The cryogenics and thermometry were identical to those of other work.[4] Two superconducting magnets enabled a few cubic centimeters of ^{3}He placed in a static field to be cooled by adiabatic demagnetization of 0.3 mole of $PrNi_5$. The sample temperature was measured by use of a ^{3}He melting-curve thermometer located in a field of about 10 G and thermally linked to the sound cell. This thermometer was in good thermal equilibrium with the sample for warming or cooling rates less than 0.6 μK/min.

The sample cell contained two X-cut quartz piezoelectric transducers spaced 1.29 cm apart which acted as an ultrasound transmitter-receiver pair. For sound propagated perpendicular to the applied field, 10-MHz fundamental crystals were used. 5-MHz transducers generated sound along the field, and the data were gathered for only one orientation at a time. rf tone bursts were applied to the transmitter, the received signal homodyne detected, and both phase components digitized by a transient recorder at 10 MHz. An on-line PDP-11/73 computer transformed these to phase and amplitude information in real time. These data were later converted into relative attenuation α and phase-velocity change $\Delta c/c$.[5] The spectrometer could resolve a 7-ppm change in velocity and a 0.05-cm^{-1} difference in α at 30 MHz.

Figure 1 shows data collected during a typical warming sweep at $\dot{T} \simeq 0.8$ μK/min from the A_2 phase for sound transmitted *orthogonal* to **H**. Because of the large $\dot{T}$, the thermometer was not in good equilibrium with the sample. This may be seen from the displacement of $T_{A_2} \simeq 2.478$ mK from its measured equilibrium value of 2.434 ± 0.002 mK. The experimental values for the temperatures of the putative normal flapping resonances are 2.426 and 2.674 ± 0.005 mK. These are to be contrasted with the theoretical results (setting $F_2^s = 0$) of 2.307 and 2.585 mK, respectively.[6–8] The discrepancies may be due to the rapid warming, but the data clearly show the splitting of the mode in a magnetic field. This is the first observation of such an effect for the normal flapping mode.[9]

The abrupt step in velocity and the peak or dip in α at T_{A_2} are anomalous for this second-order phase transition. This feature was observed only at the ultrasound signature of the A_2 transition for sound traveling perpendicular to the field. Figure 2 shows details

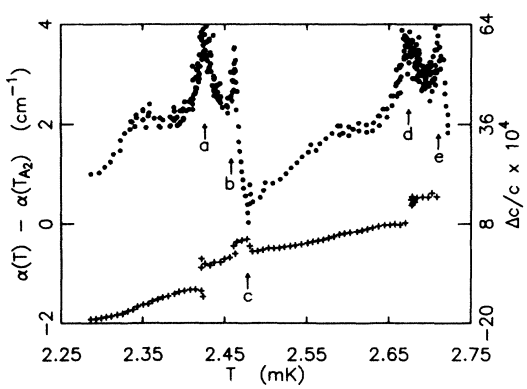

FIG. 1. Warming sweep from below T_{A_2} to just below T_{A_1} in 50 kG, 24.5 bars at 30 MHz with $\hat{\mathbf{q}} \perp \mathbf{H}$. Crosses (dots) represent velocity (attenuation) data throughout this work. The arrows indicate (from left) (a) normal flapping and (b) clapping modes in the A_2 phase, (c) T_{A_2} and its associated anomaly, and (d) normal flapping and (e) clapping modes in the A_1 phase. The receiver was saturated above T_{A_1}. The velocity jumps at the flapping modes may be inaccurate as a result of loss of signal at the absorption peaks.

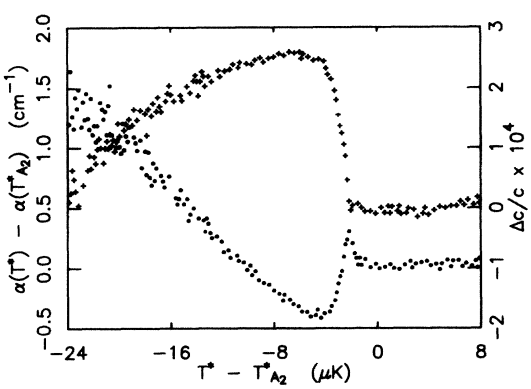

FIG. 2. Cooling through the A_2 transition in 50 kG, 24.5 bars using 30-MHz sound with $\hat{\mathbf{a}} \perp \mathbf{H}$. T^* is the pseudotime axis discussed in the text, *not* magnetic temperature.

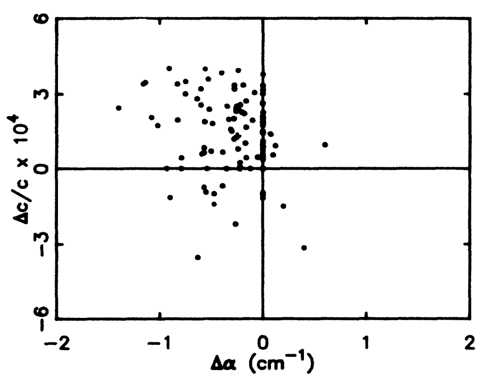

FIG. 3. A scatter plot of the changes in 30-MHz sound propagation across T_{A_2} in 50 kG and 24.5 bars. See the text for the sign conventions. The cross marks the centroid of the data at $\Delta\alpha = -0.26$ cm^{-1} and $(\Delta c/c) \times 10^4 = 1.30$. In the absence of an anomaly, all the points would fall at the origin.

of the effect at 30 MHz and 50 kG. The anomaly was detected at fields of 45, 50, 55, 65, 80, and 94 kG; for 10- and 30-MHz sound; and for both warming and cooling through T_{A_2}. All the data were collected at 24.5 bars. The thermometer's instantaneous resolution was 2 μK, limited primarily by noise in the strain-gauge capacitance bridge. To generate results such as Fig. 2, this was improved by fitting T to time with a cubic polynomial near T_{A_2}. We could not resolve the temperature at which the feature occurred from T_{A_2}, where *gradual* changes in α and $\Delta c/c$ were expected. Figure 3 illustrates the variability of the effect for fixed field, pressure, and frequency. This distribution was independent of field and frequency. We have defined $\Delta c/c = [c(T_{A_2}^-) - c(T_{A_2}^+)]/c$ and positive (negative) $\Delta\alpha$ corresponds to a rise (fall) of α on cooling through T_{A_2}. A measurement of these quantities does *not* require an *in situ* thermometer. The effect was absent not only at the A_2 transition for sound traveling along $\mathbf{H}$, but also at T_{A_1} for both orientations of $\hat{\mathbf{q}}$. Large fields are required only to separate T_{A_1} from T_{A_2}.

The anomalous nature of this observation may be seen as follows. $\Delta c/c$ and α are given by the real and imaginary parts of a density response function ξ.[2,7] Serene's mean-field calculation of ξ in the extreme collisionless limit for the $H=0$ A phase[10] may be extended to any axial phase in a finite field. The result is that $\xi = \xi_\uparrow + \xi_\downarrow$, where $\xi_\uparrow$ and $\xi_\downarrow$ are the density response functions for $\uparrow$ and $\downarrow$ spins.[2,5] This holds even if both spin-antisymmetric Landau parameters and the splitting of the density of states at the Fermi surface for the two spin directions are included. ξ_σ has a form nearly identical to that in the zero-field A phase except that Δ_σ replaces Δ throughout. Any effect which occurs at T_{A_2} but *not* at T_{A_1} is anomalous within this theory. Moreover, we expect the neglected collisions to have only a broadening action on any modes and not to engender any new phenomena unless the conditions satisfy the gapless criterion: $\Delta_\sigma < \hbar/\tau$. Here τ, the quasiparticle lifetime, is about 70 ns at a typical value for T_{A_2}.[7] ^{3}He-A_2 will be gapless for temperatures up to 0.5 μK below T_{A_2}. But gapless superfluidity cannot explain why the anomaly was observed at T_{A_2} but not at T_{A_1}, nor can it account for its geometry dependence.

Other hypothetical mechanisms may be easily eliminated. The feature cannot be a collective mode since it always occurs at T_{A_2} regardless of the applied frequency. By contrast, a collective mode falls at a temperature that is frequency dependent.[2,7] Critical-point fluctuations can be ruled out because they can account for neither a velocity jump nor a dip in attenuation. The anomaly was observed at all power levels large enough to produce a received signal, and no obvious nonlinearities were noted. The geometry dependence, the lack of an effect at T_{A_1}, and an analysis of the shapes of $\alpha(T)$ and $\Delta c(T)/c$ also preclude self-heating as an explanation.

The variable behavior of the anomaly for different crossings of T_{A_2} as well as the geometry dependence suggest a textural mechanism. Since α and $\Delta c/c$ depend on $(\hat{\mathbf{l}} \cdot \hat{\mathbf{q}})^2$ in ^{3}He-A, an abrupt change in $\hat{\mathbf{l}}$ texture at T_{A_2} would be observable for fixed $\hat{\mathbf{q}}$. Any textural change would have a negligible effect on bulk thermoydynamic properties such as specific heat jumps because the textural energies are at least 3 orders of magnitude smaller than the condensation energy at T_{A_2}.[11] The equilibrium orientation of $\hat{\mathbf{l}}$ is determined by minimization of the free-energy density $f_{\text{flow}} + f_{\text{dipole}} + f_{\text{bending}}$, subject to the boundary condition that $\hat{\mathbf{l}}$ be perpendicular to the cell walls.[12]

For the zero-field A phase, $f_{\text{flow}} \simeq 10^{-2} v_s^2 (1$

$-T/T_c)^2$ ergs/cm^3.[11] To estimate v_s we assume that it is entirely due to advection of σ, the entropy per unit mass, necessary to produce cooling or heating of the sample. Using a result from A_1-phase hydrodynamics,[13] $\rho\dot{\sigma}=\sigma\nabla\cdot\mathbf{j}_s$, gives $v_s \simeq (\dot{T}/T)(\rho/\rho_s)a$, where a is the diameter of the sound-cell fill hole. Setting $\dot{T}\simeq 1$ μK/min at T_{A_2} in 50 kG, 24.5 bars yields $v_s \sim 1.5\times10^{-5}$ cm/sec, and $f_{\text{flow}} \sim 3\times10^{-14}$ erg/cm^3. On the other hand, f_{dipole} is of order 3×10^{-5} erg/cm^3, and it orients $\hat{\mathbf{l}}\perp\hat{\mathbf{f}}$ in both ^{3}He-A_1 and -A_2 but enforces $\hat{\mathbf{l}}\parallel\hat{\mathbf{d}}$ only in the A_2 phase. That is, the texture is dipole unlocked in the A_1 phase and it is locked only in ^{3}He-A_2, where there are nonvanishing gaps for spin orientations. $\{\hat{\mathbf{d}},\hat{\mathbf{e}},\hat{\mathbf{f}}\}$ is the triad that describes the spin structure of the order parameter.[11,14] $\hat{\mathbf{f}}$ is the direction of spin pairing in the A_1 phase and $\hat{\mathbf{d}}$ is the direction along which the pairs have zero spin projection in the other phases. $\hat{\mathbf{f}}$ is pinned along $\mathbf{H}$ by susceptibility energies of order $10^{-3}[H/(1\ \text{kG})]^3$ ergs/cm^3 at T_{A_2}. Also in the Ginzburg-Landau regime,[11] $f_{\text{bending}} \simeq 8\times10^{-5}$ to 8×10^{-11} erg/cm^3, as the scale over which $\hat{\mathbf{l}}$ bends varies from the dipole bending length (~ 10 μm) to a typical sample cell dimension (~ 1 cm).

On comparing the magnitude of f_{flow} to the two other textural energies, we see that it plays a small role in these experiments. On the other hand, the observation of an attentuation anomaly near T_{A_2} by Lawson, Bozler, and Lee[3] for $\hat{\mathbf{q}}\parallel\mathbf{H}$ may have been due to significant flow in their Pomeranchuk cell. If $v_s=0$, the dipole energy forces $\hat{\mathbf{l}}\perp\mathbf{H}$, except perhaps within a dipole bending length of a wall whose normal is not perpendicular to $\mathbf{H}$. This represents a negligible (100 ppm) fraction of the total cell volume and it occupies a layer whose thickness is less than a sound wavelength. So we may assume $\hat{\mathbf{l}}\perp\mathbf{H}$ over the entire cell. The experiment can then be modeled by solving for the equilibrium planar texture over a cross section of the sound cell. We choose this section to be a square. The texture then minimizes the total dipole and bending energy in this square, with $\hat{\mathbf{l}}$ lying in the plane of the square and constrained by the usual boundary conditions at the sides. For $v_s=0$ this automatically satisfies the Mermin-Ho constraint.[15] The texture in the square is described by $\theta(x,y)$, where $\hat{\mathbf{l}}\cdot\hat{\mathbf{x}}=\cos\theta$ and $\hat{\mathbf{x}},\hat{\mathbf{y}}\perp\mathbf{H}$.

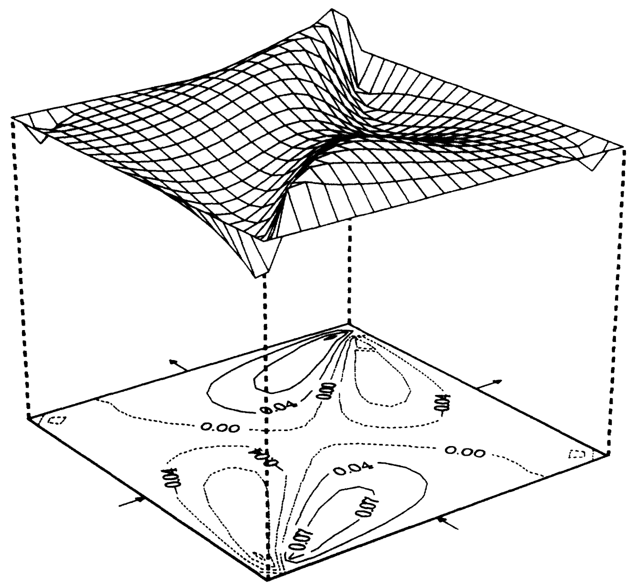

FIG. 4. The difference $\theta_{A_1}(x,y)-\theta_{A_2}(x,y)$ between orientations of an equilibrium planar texture upon crossing T_{A_2}. The contour map has peaks (valleys) outlined in solid (dashed) lines marked in radians. The boundary conditions for $\hat{\mathbf{l}}$ are shown by arrows at the sides of the map. A flat surface would indicate no change in texture at T_{A_2}.

In the A_1 phase $\hat{\mathbf{d}}$ and $\hat{\mathbf{e}}$ orient themselves in the x-y plane to be consistent with $v_s=0$, giving the total dipole-unlocked energy[5]

$$F_{A_1}=f_0\int\{(2+\cos2\theta)\theta_x^2+2\sin(2\theta)\theta_x\theta_y+(2-\cos2\theta)\theta_y^2\}dx\,dy, \tag{1}$$

where $\theta_\gamma=\partial\theta/\partial x_\gamma$ and f_0 sets the scale of f_{bending}. In the A_2 phase the dipole force will try to bring $\hat{\mathbf{d}}$ parallel or antiparallel to $\hat{\mathbf{l}}$, corresponding to longitudinal oscillation or rotation.[11] 2 μK below T_{A_2} in 50 kG and at 24.5 bars this motion has a small-amplitude frequency $f_\parallel \sim 24$ kHz. But Leggett-Takagi damping[16] will ensure that the motion lasts no more than ~ 30 msec. Therefore, the A_2-phase texture is dipole locked ($\hat{\mathbf{d}}\parallel\hat{\mathbf{l}}$), giving[5]

$$F_{A_2}=f_0\int\{5(\theta_x^2+\theta_y^2)\}dx\,dy. \tag{2}$$

The free energies (1) and (2) may be minimized by solving their Euler-Lagrange equations, which for F_{A_2} yields Laplace's equation. F_{A_1} leads to a nonlinear second-order partial differential equation which can be solved numerically by use of standard techniques.[17] Figure 4 shows the change in texture for one possible boundary condition, plotted as $\theta_{A_1}-\theta_{A_2}$ as a function of position in the square, for a 20×20 grid. The typical change in orientation of $\hat{\mathbf{l}}$ is about 0.12 rad $\simeq 7°$. The local $\alpha(x,y)$ and $\Delta c(x,y)/c$ can be calculated from these solutions, with use of[10]

$$\alpha(x,y)=\alpha_\parallel\cos^4\theta+2\alpha_c\sin^2\theta\cos^2\theta+\alpha_\perp\sin^4\theta,$$
$$\Delta c(x,y)/c=(\Delta c/c)_\parallel\cos^4\theta+2(\Delta c/c)_c\sin^2\theta\cos^2\theta+(\Delta c/c)_\perp\sin^4\theta, \tag{3}$$

TABLE I. Results of a calculation of the change in sound propagation across T_{A_2} due to the shfit in equilibrium planar texture in a square. The boundary conditions are specified as (left, bottom, right, top), and +1 (−1) denotes $\hat{\mathbf{l}}$ pointing into (out of) the area filled with ^{3}He. The third row corresponds to Fig. 4.

Boundary condition	$\alpha(T_{A_2}^-)-\alpha(T_{A_2}^+)$ (cm^{-1}) $\hat{\mathbf{q}}=\hat{\mathbf{x}}$	$\hat{\mathbf{q}}=\hat{\mathbf{y}}$	$10^4\frac{c(T_{A_2}^-)-c(T_{A_2}^+)}{c}$ $\hat{\mathbf{q}}=\hat{\mathbf{x}}$	$\hat{\mathbf{q}}=\hat{\mathbf{y}}$
(+1,+1,+1,+1)	0.171	0.158	−0.222	−0.283
(+1,+1,+1,−1)	−0.008	0.152	−0.458	0.236
(+1,+1,−1,−1)	0.233	0.256	−0.421	−0.326
(+1,−1,+1,−1)	−0.130	−0.146	0.244	0.179

where we have chosen $\hat{\mathbf{q}} \parallel \hat{\mathbf{x}}$. Taking the coefficients from Roach *et al.*[18] for 20 MHz and 26 bars, we calculate the measured α and $\Delta c/c$ by averaging the respective local quantity over the square.[19]

The results are shown in Table I, which should be compared to Fig. 3. Only the four topologically distinct solutions with minimum singularities are tabulated. A direct comparison is hampered by the lack of consistency between the experimental conditions in this work and those used to measure the coefficients in (3). Nevertheless, $|\Delta\alpha|$ is correct within the scatter of the experimental data, and the computed $|\Delta c/c|$ is several times too small. The sign of $\Delta c/c$ is determined to be opposite to that of $\Delta\alpha$, except for one case where $\Delta\alpha$ is smaller than the experimental resolution. This sign correlation is also observed in Fig. 3. These conclusions are not altered if the anisotropy coefficients of Ref. 18 are taken at $T-T_c=50$ μK, instead of the value 100 μK used above. Figure 4 and further numerical work showed that the shift in texture at T_{A_2} is not confined to the potentially troublesome corners.

In summary, we have measured anomalous behavior in sound propagation at T_{A_2} that may be qualitatively understood as a shift between dipole-locked and dipole-unlocked planar textures. This first-order transformation is driven by the second-order condensation of the minority spins, and would not occur if the minority gap were nonzero in the A_1 phase as has been recently suggested.[20]

We wish to thank Professor S. Teukolsky and Professor N. D. Mermin for stimulating discussions and Dr. D. D. Osheroff of AT&T Bell Laboratories for generously providing the Si cell filler material. This work was supported through the Cornell Materials Science Center by Grant No. DMR 8217227A-01 and was conducted on a facility jointly supported by the Cornell Materials Science Center and National Science Foundation Grant No. DMR 8418605. One of us (P.G.N. de V.) is the recipient of a National Science Foundation fellowship, 1979–1982. This work partially fulfills the requirements for the Ph.D. degree at Cornell University. Another of us (R.M.) is the recipient of an AT&T Ph.D. fellowship.

[a]Current address: AT&T Bell Laboratories, Holmdel, NJ 07733.

[1]For reviews see W. P. Halperin, Physica (Amsterdam) **109&110B&C**, 1596 (1982); P. Wölfle, Physica (Amsterdam) **1B&C**, 96 (1977).

[2]N. Schopohl, W. Marquardt, and L. Tewordt, J. Low Temp. Phys. **59**, 469 (1985).

[3]D. T. Lawson, H. M. Bozler, and D. M. Lee, Phys. Rev. Lett. **34**, 121 (1975), and in *Quantum Statistics and the Many Body Problem,* edited by S. B. Trickey, W. P. Kirk, and J. W. Dufty (Plenum, New York, 1977), p. 19.

[4]D. C. Sagan, P. G. N. de Vegvar, E. Polturak, L. Friedman, S.-S. Yan, E. L. Ziercher, and D. M. Lee, Phys. Rev. Lett. **53**, 1939 (1984); D. C. Sagan, Ph.D. thesis, Cornell University, 1985 (unpublished).

[5]P. G. N. de Vegvar, Ph.D. thesis, Cornell University, 1986 (unpublished).

[6]M. Ashida and K. Nagai, in *Proceedings of the Seventeenth International Conference on Low-Temperature Physics,* edited by U. Eckern, A. Schmid, W. Weber, and H. Wühl (North-Holland, New York, 1984), p. 783.

[7]P. Wölfle and V. E. Koch, J. Low Temp. Phys. **30**, 61 (1978).

[8]T. A. Alvesalo, T. Haavasoja, M. T. Manninen, and A. T. Soinne, Phys. Rev. Lett. **44**, 1076 (1980).

[9]R. F. Berg and G. G. Ihas, Phys. Rev. B **32**, 2851 (1985).

[10]J. W. Serene, Ph.D. thesis, Cornell University, 1974 (unpublished).

[11]A. J. Leggett, Rev. Mod. Phys. **47**, 331 (1975).

[12]D. M. Bates, S. N. Ytterboe, C. M. Gould, and H. M. Bozler, Phys. Rev. Lett. **53**, 1574 (1984).

[13]M. Liu, Phys. Rev. Lett. **43**, 1740 (1979).

[14]P. G. N. de Vegvar, Phys. Rev. B **30**, 6349 (1984).

[15]N. D. Mermin and T. L. Ho, Phys. Rev. Lett. **36**, 594, 832(E) (1976).

[16]A. J. Leggett and S. Takagi, Ann. Phys. (N.Y.) **106**, 79 (1977).

[17]W. H. Press, B. P. Flannery, S. Teukolsky, and W. T. Vetterling, *Numerical Recipes* (Cambridge Univ. Press, New York, 1985).

[18]P. R. Roach, B. M. Abraham, P. D. Roach, and J. B. Ketterson, Phys. Rev. Lett. **34**, 715 (1975).

[19]This may be rigorously justified by solving the wave equation in the presence of weak inhomogeneities with use of the Rytov technique. See L. A. Chernov, *Wave Propagation in a Random Medium* (McGraw-Hill, New York, 1960), p. 61; see also Ref. 5.

[20]H. Kojima, private communication.